

# EXPLOSIVE WELDING OF ALUMINUM TO ALUMINUM: ANALYSIS, COMPUTATIONS AND EXPERIMENTS

F. Grignon, D. Benson, K. S. Vecchio and M. A. Meyers

*Department of Mechanical and Aerospace Engineering  
University of California, San Diego, La Jolla, CA 92093*

**Abstract.** 6061 T0 aluminum alloy was joined to 6061 T0 aluminum alloy by explosive welding. This is a process in which the controlled energy of a detonating explosive is used to create a metallic bond between two similar or dissimilar materials. The welding conditions were tailored to produce both wavy and straight interfaces. A three-pronged study was used to establish the conditions for straight weld formation: (a) analytical calculation of the domain of weldability; (b) characterization of the explosive welding experiments carried out under different conditions, and (c) 2D finite differences simulation of these tests using the explicit Eulerian hydrocode Raven with a Johnson-Cook constitutive equation for the Al alloy. The numerical simulation and the analytical calculations confirm the experimental results and explain the difficulties met for obtaining a continuous straight interface along the entire weld.

## INTRODUCTION

The Mars Sample Return Mission planned for the future will use a capsule to collect soil samples. This capsule will be hermetically sealed on Mars prior to the return mission in order to avoid contamination upon return to Earth. A novel containerization technique that satisfies the Planetary Protection Category V requirements has been developed at the Jet Propulsion Laboratory [1]. The proposed approach uses explosive welding, which possesses several characteristics that are important for the planetary protection compliant containerization. The main disadvantage of the explosive welding process, from a planetary protection point of view, is the propensity of the bond to form interface waves that may prevent ejecta (Fig. 1) from completely leaving the bonded area and trap some surface particles within these waves.

The objective of the research program, whose results are described herein, was to determine the right welding parameters for providing the smoothest interface.

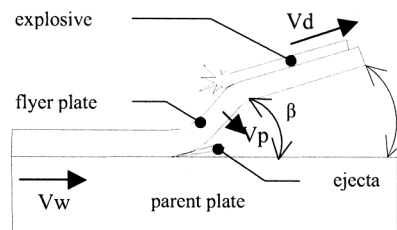


FIGURE 1. Explosive welding process

## ANALYSIS

### Weldability window

A large number of scientists worked on the understanding of the subject and Crossland [2] wrote a complete monograph on the process. The achieved work enables the construction of a plot that Szecket [3] named the "weldability window", which includes both a straight and wavy interface domain. This plot is applied to the 6061 T0 aluminum alloy used in this investigation. Known values of  $\alpha$ ,  $\beta$ ,  $V_d$ ,  $V_p$ ,  $V_w$

(Fig. 1) and the properties of the material enable the design of the weldability window.  $V_p$  is calculated from the Gurney equation [4], which only predicts a terminal velocity; the problem of the flyer plate acceleration is intentionally left out. Equation 1 gives the lower limit for welding;  $\beta$  is in radians,  $k_1$  is a constant,  $H$  is the Vickers hardness in  $N/m^2$ , and  $\rho$  is the density in  $kg/m^3$ . The value of  $k_1$  is 0.6 for high quality pre-cleaning of surfaces, and 1.2 for imperfectly cleaned surfaces. Equation 2 gives the upper limit for welding.  $k_3$  should be evaluated experimentally at a value of  $V_w$ , which is equal to half of the compressive wave velocity  $C_f$  ( $V_w=2645m/s$  for pure aluminum).

$$\beta = k_1 \cdot \sqrt{\frac{H}{\rho \cdot V_w^2}} \quad (1)$$

$$\sin \frac{\beta}{2} = \frac{k_3}{t^{0.25} \cdot V_w^{1.25}} \quad (2)$$

Equation 3, due to Szecket [5], gives the smooth-wavy transition zone for the 2024 Al alloy. This zone has been built with experimental results. Szecket developed a weldability zone, which contained left and right boundaries.

$$R_i = 122.32(\pm 16.9) - 19.35(\pm 3.65)\beta + 1.07(\pm 0.24)\beta^2 - 0.020(\pm 0.005)\beta^3 \quad (3)$$

Szecket's results for 2024 Al are merged with data for the 6061 T0 aluminum alloy used in this investigation. Specific parameters are:  $\rho=2700 kg/m^3$ ;  $H_v=38 kg/mm^2$ ;  $C_f=5293m/s$ . The transition zone is given for the 2024 aluminum alloy; nevertheless, the parameters corresponding to the lower limit for less perfectly cleaned surfaces ( $V_w=3000m/s$  to  $V_w=5000m/s$ ) should enable a welding without waves. These values correspond to the collision angles  $\beta$  between  $9^\circ$  and  $15^\circ$ . If PETN and a value of  $R=1/3$  are chosen, the range of the initial angle  $\alpha$  will be from  $5^\circ$  to  $10^\circ$ . Figure 2 shows the application of Equations 1-3 to the  $V_w$  vs.  $\beta$  space. Two different flyer plate thicknesses  $t$  are used: 1.5 and 3 mm. The smooth-wavy interface transition is shown in this plot, and two regimes are clearly seen.

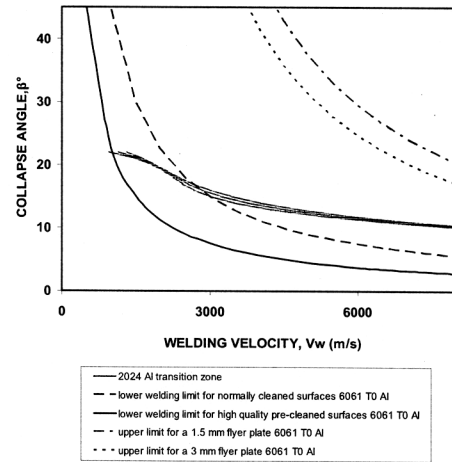


FIGURE 2. Weldability window of 6061T0 Al alloy.

## EXPERIMENTS

### Experimental set-up

Figure 3 shows the proposed capsule used in Mars Sample Return Mission. In order to experiment with these conditions, flat plates were tested. Indeed, it has been shown that the axial collapse and not the radial propagation is responsible for welding. The radial velocity is supersonic with respect to aluminum and therefore cannot promote welding. Thus, the problem was reduced to two dimensions in order to become tractable. The experimental set-up uses a chamfered parent plate in order to facilitate the creation of the initial angle  $\alpha$ . These experiments have been performed with  $\alpha$  varying between  $4^\circ$  and  $14^\circ$ . A PETN-based plastic explosive was used with a linear density of  $4.25 g/m$ .

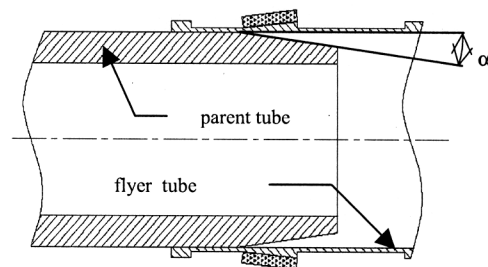
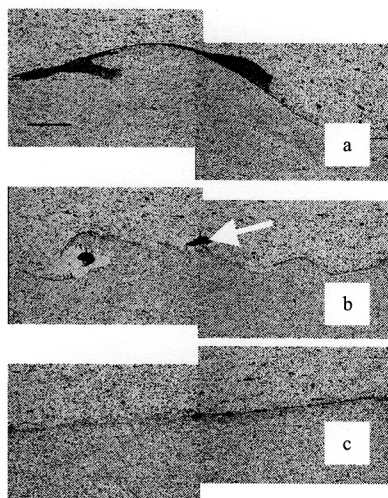


FIGURE 3. Capsule, tube to tube welding.

## Results

Experiments were carried out at initial angles of 4, 6, 8, 10, 12 and 14°. Figure 4 shows details from the initial, middle, and final portions of the weld for  $\alpha = 10^\circ$ . Welding was initiated at the top left and terminated at the bottom right. The weld morphology is initially wavy (first 1/3) and then becomes smooth. The same pattern was observed for the other values of  $\alpha$ . There are clear differences between the wavelengths of the welds for the different values of  $\alpha$ . Simple theoretical considerations assume (and this is the main assumption of the analytical treatment) that explosive welding is a steady process, even at values of  $\alpha$  different from zero. This means that, for fixed initial parameters, the interfacial geometry retains the same shape along the length of the weld. However, Fig. 4 shows that there is no stable interfacial geometry. The white arrow shows a void due to solidification shrinkage. The presence of voids from solidification shrinkage and the lower wavelength on the right are evidence of increased melting.



**FIGURE 4.** Weld interface for initial angle  $\alpha = 10^\circ$  using Au tracer at interface; (a) initial portion; (b) transition portion; (c) final portion.

## FINITE ELEMENT MODELING

Finite element simulations were carried out using the explicit Eulerian hydrocode Raven [6]. The Johnson-Cook constitutive model was used for the 6061 T0 aluminum alloy, and JWL EOS was used for the explosive. Figure 5 shows that the angle  $\beta$  is not constant; rather, it increases with time. This is an important result, and it is consistent with the metallographic characterization of the weld morphology reported in the experiments. It should also be noted that the thickness of the flyer plate is not constant either, contrary to the assumptions made until now.

From the simulations it is possible to obtain the relationships between  $\beta$  and time,  $V_p$  and time and then,  $\beta$  and  $V_p$ . The results of these measurements are shown in Fig. 6 for three values of the initial angle  $\alpha$  (4, 8, and  $10^\circ$ ). The Szecket plot is superimposed on the same figure. The interfacial weld morphology is initially wavy for the three angles. As the collision angle  $\beta$  increases (and this angle increases with time, as shown in Fig. 5) the wavy-smooth boundary is traversed for the three cases. From that point on the welding interface is smooth. Again, this is in full agreement with the observations made in the experiments.

The computations also show that the smaller  $\alpha$ , the more rapid is the increase of  $\beta$  and  $V_p$ . For  $\alpha = 4^\circ$ , the interface has a very short smooth-wavy transition part, and the wavelength is not constant. For  $\alpha = 8^\circ$ , the interface has a large smooth-wavy transition part, and its wavelength should not be constant.

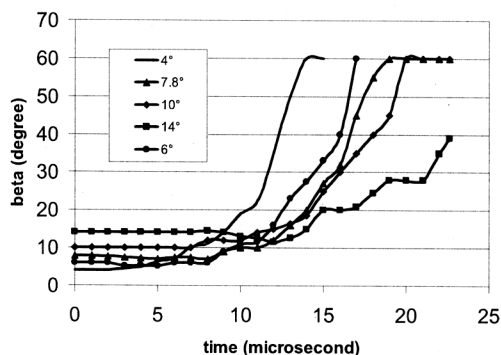


**FIGURE 5.** Computed collision angle as a function of time for different values of  $\alpha$ .

Furthermore, the transition zone is reached earlier than for  $\alpha=4^\circ$ . For  $\alpha=10^\circ$ , the wavy part might be divided in two zones: the first one with decreasing wavelength as in  $\alpha=4^\circ$  and  $\alpha=8^\circ$ , the second one with constant wavelength. The transition region is larger than for  $4^\circ$  but shorter than for  $8^\circ$ . These predictions from the numerical results are confirmed by the experimental observations. Note also, in regard to the wave shapes, that the wavelength depends on the impact velocity  $V_p$  whereas the amplitude depends on the initial angle  $\alpha$ . Melting appears when  $V_p$  is constant during a few microseconds.

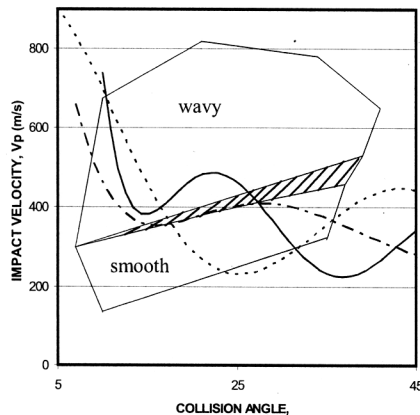


FIGURE 6. Interfacial geometry as a function of the initial angle  $\alpha$  in the  $\beta$  vs.  $V_p$  plane.

### CONCLUSIONS

The objective of this study was to establish the conditions for straight, smooth weld formation in the explosive welding of 6061T0 vs. 6061T0. The smooth and straight domains defined by Szecket [5] were used to successfully predict the two regimes. Szecket's [5] results for 2024 Al were supplemented by the constitutive response for 6061T0 and yielded a plot applicable to the experimental results containing both wavy and smooth domains. The present results follow Szecket's [5] calculation made for the 2024 aluminum alloy. It was possible to calculate the relationship between the terminal velocity  $V_p$  and the flyer thickness with the Gurney equation. The agreement between the calculation and the computational simulation proves that the

assumption made on the flyer plate acceleration is reasonable. Experimental observations (by optical microscopy) on explosively welded specimens suggested that the  $V_p$ - $\beta$  relation was not constant during the welding process since, in all cases, a region of wavy weld was followed by smooth weld. The thickness of the materials influences the welding process and consequently the collision angle  $\beta$ . For the configuration chosen for the capsules in the Mars Return Mission, the flyer plate thickness is not a constant, and thus, the impact velocity  $V_p$  should vary.

Finite element calculations were conducted in a two-dimensional geometry. From a numerical point of view, the results are particularly convincing. Although the individual wave formation could not be monitored because of mesh size limitations, the results demonstrate that the collision angle increases with propagation distance for all initial configurations analyzed. This change in collision angle is directly responsible for the change in interface morphology from wavy to smooth at the welding front. Furthermore, the correlation between the experiments and the simulations demonstrates that the model is good enough to simulate the process.

### ACKNOWLEDGEMENT

The funding of this program by the Jet Propulsion Laboratory through Dr. Mark Adams is gratefully acknowledged. Frequent discussions with Dr. Benjamin Dolgin and Joseph Sanok are greatly appreciated.

### REFERENCES

1. Dolgin B, Sanok J, Sevilla D and Bement L. Category V compliant container for Mars Sample Return Missions. 00ICES-131 2000
2. Crossland B. Explosive Welding of Metals and its Applications. Oxford: Oxford Science Publication 1982.
3. Jaramillo D, Szecket A, Inal O.T. On the transition from a waveless to a wavy interface in explosive welding. Materials Science and Engineering 1987;91:217-222.
4. Meyers M.A. Dynamic Behavior of Materials. Wiley Interscience 1994.
5. Szecket A, Mayseless M. The triggering and controlling of stable interfacial conditions in explosive welding. Materials Science and Engineering 1983;57:149-154.
6. Benson D.J. RAVEN: User's Manual ver 2000.

